Development of the SAPRC-07 chemical mechanism

William P.L. Carter

College of Engineering Center for Environmental Research and Technology and Air Pollution Research Center, University of California, Riverside, CA 92521, USA

A R T I C L E   I N F O

A B S T R A C T

An updated version of the SAPRC-99 gas-phase atmospheric chemical mechanism, designated SAPRC-07, is described. The rate constants and reactions have been updated based on current data and evaluations, the aromatics mechanisms have been reformulated and are less parameterized, chlorine chemistry has been added, the method used to represent peroxy reactions has been reformulated to be more appropriate for modeling gas-phase secondary organic aerosol precursors, and representations for many types of VOCs have been added or improved. This mechanism was evaluated against the result of $\sim$2400 environmental chamber experiments carried out in 11 different environmental chambers, including experiments to test mechanisms for over 110 types of VOCs. The performance in simulating the chamber data was generally satisfactory for most types of VOCs but some biases were seen in simulations of some types of experiments. The mechanism was used to derive updated MIR and other ozone reactivity scales for almost 1100 types of VOCs, though in most cases the changes in MIR values relative to SAPRC-99 were not large. This mechanism update results in somewhat lower predictions of ozone in one-day ambient model scenarios under low VOC/NO$_x$ conditions. The files needed to implement the mechanism and additional documentation is available at the SAPRC mechanism web site at http://www.cert.ucr.edu/~carter/SAPRC.

1. Introduction

Airshed models are essential for the development of effective control strategies for reducing photochemical air pollution because they provide a scientific basis for making quantitative estimates of changes in air quality resulting from changes in emissions. The gas-phase chemical mechanism is an important component of such models that represents the processes by which emitted volatile organic compound (VOC) pollutants and oxides of nitrogen (NO$_x$) react to form secondary pollutants such as ozone (O$_3$) and other oxidants. Examples of mechanisms used in current airshed models, listed in approximate order of development, are Carbon Bond 4 (Gery et al., 1988), RADM-2 (Stockwell et al., 1990), RACM (Stockwell et al., 1997), SAPRC-99 (Carter, 2000a,b), MCM (Jenkin et al., 1997, 2003; Saunders et al., 2003), and Carbon Bond 05 (Yarwood et al., 2005; Sarwar et al., 2008).

Another airshed model application where the accuracy of the chemical mechanism is important is the calculation of reactivity scales that measure relative impacts of different types of VOCs on ozone formation. The current California Air Resources Board (CARB) regulations (CARB, 1993, 2000) use the Maximum Incremental Reactivity (MIR) scale calculated using the SAPRC-99 chemical mechanism (Carter, 2000a, 2003) that was developed in part for this

purpose. The MCM is the only other available mechanism that has been used for developing comprehensive VOC reactivity scales (e.g., Derwent et al., 1998); the other mechanisms cited above are too condensed to be suitable for this purpose.

The SAPRC-99 mechanism includes representations of atmospheric reactions of almost 780 types of VOCs for reactivity assessment, and is widely used in other airshed modeling applications. Although this represented the state of the art at the time it was developed (Stockwell, 1999), there has been continued progress in basic atmospheric chemistry, and new information has become available concerning the reactions and O$_3$ impacts of many individual VOCs. There was also a desire to add chlorine chemistry to the mechanism (e.g., see Tanaka et al., 2003). In view of this, the CARB funded the development of the SAPRC-07 mechanism as an update to SAPRC-99, for use in airshed models and to update the MIR scale. This updated mechanism, its evaluation against chamber data, and the updated reactivity scales and ozone predictions are summarized in this paper. More detailed information and documentation, and files implementing the mechanism, are available in the final report for this project and at the SAPRC mechanism web site (Carter, 2010a,b).

2. Mechanism structure

The SAPRC-07 mechanism, like SAPRC-99, is modular in structure and different portion can be used depending on the application. The *base mechanism* represents the reactions of the inorganic

E-mail address: carter@cert.ucr.edu.

species, the common organic products, and the intermediate radicals leading to these products, including those formed from the initial reactions of the represented VOCs not in the base mechanism. The reactions of inorganic chlorine species and model species used to represent chlorine-containing organic products are in the *base chlorine mechanism*, which is new to SAPRC-07 and is only needed if chlorine species are to be modeled. These include reactions of a few emitted VOC that are important and not amenable to lumping with other species (see Table 1). However, most other VOCs are represented in separate modules containing either in mechanisms of individual VOCs or mechanisms for lumped model species used in airshed models.

The SAPRC mechanisms have the ability to optionally include separate representations of the reactions of hundreds of different types of VOCs. Generally these are not all included in the airshed model at the same time, but selected compounds can be represented separately for the purpose of calculating reactivity scales or for toxics modeling, or mechanisms for groups of compounds can be used to derive parameters for the lumped model species used for representing complex mixtures such as ambient emissions. The SAPRC-07 mechanism now has separate representations for 748 types of VOCs, making it the most comprehensive in terms of numbers of types of VOCs than any current gas-phase atmospheric mechanism. These mechanisms are derived either by using a chemical mechanism generation and estimation software system or by compound-specific considerations as discussed below. In addition, for deriving reactivity scales or representing complex mixtures, 320 additional types of VOCs are represented using the "lumped molecule approach", where their impacts are estimated by assuming they are the same, on a per-molecule basis, of a separately represented compound (Dodge, 2000; Carter, 2010a). This approximation is used in these cases because of insufficient mechanistic information, expected similarity to other species, or judgments of relatively lower importance in emissions.

The mechanisms for the individual VOCs are used, in conjunction with an ambient VOC mixture taken as representative, to derive mechanisms for the 10 lumped model species that are used in most airshed model applications to represent these VOCs (see Table 1). Two modules are available for the *lumped model species* mechanisms, one suitable for use in models without chlorine chemistry, and the other containing their reactions with chlorine atoms.

3. Base mechanism

The species included in the base and the base chlorine mechanisms are listed in Table 1, and their reactions and rate parameters are given in Table A-1 and Table A-2 in the Supplementary Materials. Footnotes to the tables in the supplementary materials document the reactions and rate constants used. Absorption cross-sections and quantum yields for the photolysis reactions are given in Table A-3. Most of the individual VOCs are represented separately from the base mechanism, as discussed in the next section.

Except for the addition of the chlorine species and changes made to the peroxy radical representation and aromatics mechanisms as discussed below, most of the model species in this base mechanism are the same as in SAPRC-99. Phenol is now lumped with cresols since its separate representation was not found to have a significant effect on model simulations of benzene experiments or ambient mixtures. The HO_2 + formaldehyde adduct species was removed because it was found to have no effect model simulations of interest. Formic acid, acetic acid, and the lumped higher organic acids, previously treated as inert tracers, were added to the base mechanism as reactive species, to improve the representation of organic acids in models for long-range transport. In addition, benzene and acetylene are now represented explicitly in the base

mechanism because these two compounds are relatively important in emissions and their reactivities are quite different than the other compounds with which they previously were lumped.

The updates to the mechanism included potentially significant changes in some rate constants. Selected potentially important rate constant changes are listed in Table 2. Sensitivity studies (e.g., Bergin et al., 1999), have shown that the NO_2 photolysis rate, the rate constant for the reaction of OH with NO_2, and reactions involving formation of PAN species are all important in affecting predicted O_3 concentrations, and changes have been made regarding all these reactions. The glyoxal and methylglyoxal photolysis rates were increased, but other changes were to the aromatics mechanisms that may offset these increases, so the significance of these changes by themselves is not clear. The methacrolein and formaldehyde photolysis rates were increased somewhat, but the photolysis rate for the model species used to represent the higher ketone products was decreased significantly because of lower apparent photolysis rates for higher ketones derived from modeling chamber experiments with such compounds (see footnotes to tables in the Supplementary Materials). Rate constants involving hydroperoxide formation from the reaction of peroxy radicals with HO_2 decreased significantly, though reaction with HO_2 is still calculated to be the major sink for peroxy radicals once NO_x is depleted. The reasons for the changes in these rate constants or photolysis rates are discussed in footnotes to and Table A-2 in the Supplementary Materials.

Except for the updated rate constants and photolysis data, the base inorganic chlorine mechanism is very similar to that developed previously by Carter et al. (1997). The major difference is the addition of separate model species to represent the reactions of chlorinated aldehydes and ketones that may be formed in the reactions of chlorinated VOCs. Carter and Malkina (2007) found that the reactivities of the 1,3-dichloropropenes are significantly underpredicted if the standard aldehyde model species are used to represent the reactions of the chloroacetaldehyde predicted to be formed, but satisfactory simulations are obtained if a separate model species is used, using the NASA (2006)-recommended absorption cross-sections and quantum yields for this compound, which gives photolysis rates that are ∼4.5 times faster than the lumped higher aldehyde model species used in the standard base mechanism. This chloroacetaldehyde model species is also used to represent the reactions of other α-chloroaldehydes, which are assumed to be similarly photoreactive. Because chloroacetone is calculated to photolyze ∼7 times faster than MEK and even more for higher ketones, a chloroacetone model species is added to represent the reactions of α-chloroketones.

Because of the large number of peroxy radicals that are involved even in condensed atmospheric chemistry mechanisms, SAPRC-99 uses a limited number of "chemical operators" to represent effects of peroxy radical reactions on NO_x and radicals, and represents the organic products formed when peroxy radicals (other than methyl peroxy) react with other peroxy radicals by those formed when they react with NO_x. Use of this condensed representations of peroxy radical reactions, which is also employed in the Carbon Bond 4 (Gery et al., 1988) and Carbon Bond 05 mechanisms (Yarwood et al., 2005), has been shown to have relatively little effects on predictions of O_3 formation and overall gas-phase reactivity because they involve no approximation when the major fate of peroxy radicals is reaction with NO, as is the case when O_3 formation occurs, and because they give reasonably good representations of how NO_x conversions and radical regenerations change when NO_x levels are reduced. However, this approximation does not account for the changes in organic oxidation products that occur when these peroxy + peroxy reactions become non-negligible, since they use the set of products formed in the peroxy + NO reaction as surrogates for the generally different products formed under low NO_x conditions. Recent environmental

Table 1
List of model species used in the mechanism.

Name	Description
Base Mechanism	
Constant Species	
O2	Oxygen
M	Air
H2O	Water
H2	Hydrogen molecules
HV	Light (optionally can be used to scale all photolysis rates)
Active Inorganic Species	
O3	Ozone
NO	Nitric oxide
NO2	Nitrogen dioxide
NO3	Nitrate radical
N2O5	Nitrogen pentoxide
HONO	Nitrous acid
HNO3	Nitric acid
HNO4	Peroxynitric acid
HO2H	Hydrogen peroxide
CO	Carbon monoxide
SO2	Sulfur dioxide
Active Radical Species and Operators	
OH	Hydroxyl radicals
HO2	Hydroperoxide radicals
MEO2	Methyl peroxy radicals
RO2C	Peroxy radical operator representing NO to NO_2 and NO_3 to NO_2 conversions, and the effects of peroxy radical reactions on other species
RO2XC	Peroxy radical operator representing NO consumption (used in conjunction with organic nitrate formation), and the effects of peroxy radical reactions other species
MECO3	Acetyl peroxy radicals
RCO3	Peroxy propionyl and higher peroxy acyl radicals
BZCO3	Peroxyacyl radical formed from aromatic aldehydes
MACO3	Peroxyacyl radicals formed from methacrolein and other acroleins
Steady State Radical Species	
O3P	Ground state oxygen atoms
O1D	Excited oxygen atoms
TBUO	t-Butoxy radicals
BZO	Phenoxy radicals
PAN and PAN Analogues	
PAN	Peroxy acetyl nitrate
PAN2	PPN and other higher alkyl PAN analogues
PBZN	PAN analogues formed from aromatic aldehydes
MAPAN	PAN analogue formed from methacrolein
Reactive Organic Product Species	
HCHO	Formaldehyde
CCHO	Acetaldehyde
RCHO	Lumped C_3 + aldehydes. Mechanism based on propionaldehyde
ACET	Acetone
MEK	Ketones and other non-aldehyde oxygenated products whose OH radical rate constants are between 5×10^{-13} and 5×10^{-12} cm^3 mol^{-2} s^{-1}. Based on methyl ethyl ketone
PROD2	Ketones and other non-aldehyde oxygenated products whose OH radical rate constants are greater than 5×10^{-12} cm^3 mol^{-2} s^{-1}. Based on higher ketones formed from alkanes
RNO3	Lumped organic nitrates. Based on organic nitrates formed from alkanes
MEOH	Methanol
HCOOH	Formic acid
CCOOH	Acetic acid. Also used for peroxyacetic acid.
RCOOH	Higher organic acids and peroxy acids. Mechanism based on propionic acid.
COOH	Methyl hydroperoxide
ROOH	Lumped organic hydroperoxides with 2–4 carbons. Based n-propyl hydroperoxide.
RAOOH	Organic hydroperoxides formed following OH addition to aromatic rings
R6OOH	Other lumped organic hydroperoxides with 5 or more carbons
GLY	Glyoxal
MGLY	Methylglyoxal
BACL	Biacetyl
CRES	Phenols and cresols. Mechanism based on o-cresol.
NPHE	Nitrophenols
BALD	Aromatic aldehydes. Mechanism based on benzaldehyde
MACR	Methacrolein
MVK	Methyl vinyl ketone
IPRD	Lumped isoprene product species (Carter and Atkinson, 1996)

Table 1 (*continued*)

Name	Description
Aromatic unsaturated ring fragmentation products (see discussion of aromatic mechanisms)	
AFG1	Lumped monounsaturated dicarbonyl aromatic products that photolyze to form radicals
AFG2	Lumped monounsaturated dicarbonyl products that photolyze to form non-radical products
AFG3	Lumped diunsaturatred dicarbonyl aromatic products that do not photolyze
Steady state operators used to represent radical or product formation in peroxy radical reactions	
x(Prod)	Formation of product "Prod" from alkoxy radicals formed in peroxy radical reactions with NO and NO_3 (100% yields) and RO_2 (50% yields). Separate species for all reactive radicals and products ultimately formed from peroxy radical reactions
zRNO3	Formation of RNO3 in the $RO_2 + NO$, reaction, or formation of corresponding non-nitrate products (represented by PROD2) formed from alkoxy radicals formed in $RO_2 + NO_3$ and (in 50% yields) $RO_2 + RO_2$ reactions
y(Prod)	Formation of a hydroperoxide product following $RO_2 + HO_2$ reactions, or formation of H-shift disproportionation products in the $RO_2 + RCO_3$ and (in 50% yields) $RO_2 + RO_2$ reactions. Separate species for ROOH, R6OOH, and RAOOH
Non-Reacting Species	
CO2	Carbon dioxide
SULF	Sulfates (SO_3 or H_2SO_4)
XC	Lost carbon or carbon in unreactive products
XN	Lost nitrogen or nitrogen in unreactive products
Primary Organics Represented Separately in the Base Mechanism	
CH4	Methane
ETHENE	Ethene
ISOPRENE	Isoprene
ACETYLEN	Acetylene
BENZENE	Benzene
Base Chlorine Mechanism	
Inorganic Species	
CL2	Chlorine molecules
CL	Chlorine atoms
HCL	Hydrochloric acid
CLNO	ClNO
CLONO	ClONO
CLNO2	$ClNO_2$
CLONO2	$ClONO_2$
HOCL	HOCl
CLO	$ClO^\bullet$ radicals
Organic Product Species	
CLCCHO	Chloroacetaldehyde and other alpha-chloro aldehydes
CLACET	Chloroacetone and other alpha-chloro ketones
CLCHO	Formyl Chloride (assumed to be unreactive)
Lumped model species added to the base mechanism to represent emitted species in the lumped mechanism for airshed models	
ALK1	Alkanes and other non-aromatic compounds that react only with OH, and have kOH (OH radical rate constant) between 2 and 5×10^2 ppm^{-1} min^{-1}. (Primarily ethane)
ALK2	Alkanes and other non-aromatic compounds that react only with OH, and have kOH between 5×10^2 and 2.5×10^3 ppm^{-1} min^{-1}. (Primarily propane)
ALK3	Alkanes and other non-aromatic compounds that react only with OH, and have kOH between 2.5×10^3 and 5×10^3 ppm^{-1} min^{-1}.
ALK4	Alkanes and other non-aromatic compounds that react only with OH, and have kOH between 5×10^3 and 1×10^4 ppm^{-1} min^{-1}.
ALK5	Alkanes and other non-aromatic compounds that react only with OH, and have kOH greater than 1×10^4 ppm^{-1} min^{-1}.
ARO1	Aromatics with kOH $< 2 \times 10^4$ ppm^{-1} min^{-1}.
ARO2	Aromatics with kOH $> 2 \times 10^4$ ppm^{-1} min^{-1}.
OLE1	Alkenes (other than ethene) with kOH $< 7 \times 10^4$ ppm^{-1} min^{-1}.
OLE2	Alkenes with kOH $> 7 \times 10^4$ ppm^{-1} min^{-1}.
TERP	Terpenes

chamber studies (Odum et al., 1996, Hurley et al., 2001, Sato et al., 2004; Song et al., 2005) indicate that SOA formation can change significantly with VOC/NO_x ratios. This is attributed to competing branching ratios in reactions of peroxy radicals with NO_x, HO_2, and other peroxy radicals.

Therefore, the peroxy radical representation was changed as part of this update. Like SAPRC-99, the SAPRC-07 representation uses operators to represent the effects of peroxy radicals on NO_x, with "RO2C" representing NO to NO_2 conversions and "RO2XC" representing NO consumption that occurs in conjunction with nitrate formation, but unlike SAPRC-99 it uses separate chemical operator model species to represent the formation of each of the radicals and

oxidation products, and how they depend on which peroxy radical reactions are occurring. Three sets of chemical operators are used for this purpose: "xPROD" species are used to represent the formation of the alkoxy radical products resulting when the peroxy radical react with NO, NO_3, and (in part) RO_2; "yPROD" species are used to represent the formation of hydroperoxides formed when peroxy radicals react with HO_2 or H-shift disproportion products formed when peroxy radicals react with acyl peroxy radicals or (in part) with RO_2; and "zRNO$_3$" species are used to represent the formation of organic nitrates when peroxy radicals react with NO or the alkoxy radical formed (in part) in $RO_2 + RO_2$ reactions. The products formed in the reactions of these operators are summarized on Table A-4 in

Table 2
Selected potentially important rate constant changes in the updated mechanism relative to SAPRC-99.

Rate constant or photolysis rate[a]			Reaction
SAPRC-99	SAPRC-07	Change	
6.69E−01	7.23E−01	8%	$NO_2 + HV = NO + O3P$
8.81E−12	1.05E−11	19%	$OH + NO_2 = HNO3$
5.12E−12	4.65E−12	−9%	$MEO_2 + HO_2 = COOH + O_2$
1.45E−11	7.63E−12	−47%	$Peroxy + HO_2 = products$
1.04E−11	9.37E−12	−10%	$MECO_3 + NO_2 = PAN$
7.04E−04	6.27E−04	−11%	$PAN = MECO_3 + NO_2$
(Omitted)	6.12E−05		$PAN + HV = Products$
2.12E−11	1.97E−11	−8%	$MECO_3 + NO = MEO_2 + CO_2 + NO_2$
5.90E−04	5.48E−04	19%	$PAN2 = RCO_3 + NO_2$
2.78E−11	2.08E−11	−34%	$RCO_3 + NO = NO_2 + products$
2.32E−03	2.76E−03	16%	$HCHO + HV = 2HO_2 + CO$
1.08E−03	3.18E−03	88%	$GLY + HV = HCHO + CO$
1.10E−02	1.56E−02	30%	$MGLY + HV = products$
1.36E−04	1.97E−04	31%	$MACR + HV = products$
1.90E−05	4.69E−06	−304%	$PROD2 + HV = products$

[a] Thermal rate constants are for $T = 300$ K and are in molecule, $cm^3 s^{-1}$ units. Photolysis rates are in s^{-1} and are calculated for direct overhead sunlight based on the actinic fluxes used in the reactivity scale calculations (Carter, 1994a,b). Change is (SAPRC-07 − SAPRC-99)/SAPRC-99.

the Supplementary Materials, and Table A-1 and its footnotes indicate how they are implemented in the model.

4. Mechanisms for individual VOCs

A listing of all of the types of VOCs that can be separately represented in the current mechanism is given in Table A-5 in the Supplementary Materials, and Table A-6 lists those VOCs that have been evaluated against environmental chamber data. Table A-5 also indicates the type of mechanisms and how they were derived, gives the OH radical rate constants used for all the VOCs and how they were derived, their calculated atmospheric ozone reactivities in selected scales (discussed below), and subjective mechanism bias and uncertainty classifications for ozone predictions. For the VOCs evaluated against chamber data, Table A-6 gives the number of runs of various types used to evaluate the mechanisms, codes indicating adjustments made to the mechanisms (if any) based on the simulations of the data, and statistics measuring the ability of the mechanism to simulate O_3 formed and NO oxidized in the experiments, as discussed below. The full mechanisms for all these VOCs are given by Carter (2010a,b). The various types of mechanisms are summarized below.

4.1. Mechanism generation system

As indicated in footnotes to Table A-5, the mechanisms for many of the VOCs, including alkanes, and most alkenes, oxygenates and organic nitrates, were derived using the automated mechanism generation and estimation software system that is described in the SAPRC-99 documentation (Carter, 2000a), with updates for SAPRC-07 (Carter, 2010a). Given the structure of the molecule, available information concerning applicable rate constants and branching ratios, and various estimation methods, this system can derive fully explicit mechanisms for the atmospheric reactions of many classes of VOCs in the presence of NO_x, and then use these mechanisms to derive the appropriate representations of the VOCs in terms of the model species in the base mechanism. If rate constant or relevant branching ratio data are available for the compound, or parameters had to be adjusted based on fits to the chamber data (as discussed below), then the measured or adjusted values were used in place of the estimates. Further discussion of this system is beyond the scope of this paper (see Carter, 2000a, 2010a).

4.2. Benzene and alkylbenzene mechanisms

The mechanisms for aromatics could not be derived using the mechanism estimation system because insufficient information exists concerning their reactions for deriving predictive and explicit mechanisms based on mechanistic considerations alone. However, progress has been made in recent years concerning the atmospheric reactions of aromatics and their reactive products (e.g., Calvert et al., 2002; Barnes, 2006, and references therein), allowing derivation of potentially more chemically realistic mechanisms than the simplified parameterized representation used in SAPRC-99 (Carter, 2000a). The general model we assume for the ring-opening reactions of benzene and the alkylbenzenes, which is still almost certainly an oversimplification of what really happens because the actual distribution of products appears to be more complex (Calvert et al., 2002), is shown in Fig. 1a, using benzene as an example. The processes are assumed to be analogous for the substituted benzenes such as toluene, xylenes, etc., except that the number of reactions and products are greater, and reactions at the alkyl substituents, such as shown on Fig. 1b using toluene as the example, can also occur.

The aromatic products whose yields have been quantified include the phenols and cresols, the α-dicarbonyls (phenol and glyoxal in the case of benzene), and the ring containing products, such as benzaldehyde, formed from reactions at the alkyl groups. The formation of phenols is assumed to occur as shown on Fig. 1a as "A". The processes forming the α-dicarbonyls are more uncertain and are assumed to occur as shown as "B". The predicted co-products are the mono-unsaturated 1,4-dicarbonyls, e.g., 2-butene 1,4-dial. These products are indeed observed (Calvert et al., 2002, and references therein; Arey et al., 2009), though the measured total yields are generally much less than the total α-dicarbonyl yields. This could be due to other, unknown, processes leading to the α-dicarbonyls, or with problems with quantifying these highly reactive compounds. For lack of available information we assume the latter is the case. Process "B" involves the intermediacy of peroxy radicals that convert NO to NO_2, react with NO to form organic nitrates ("C" on Fig. 1a), react with HO_2 to form a highly oxygenated bicyclic hydroperoxide ("D" on Fig. 1a), or react with other peroxy radicals to form other products (not shown on the figure). The hydroperoxides formed in the HO_2 reaction (e.g., "D") are represented by a separate model species RAOOH because they may to have higher PM formation potential than other hydroperoxides because of their high oxygen content, though the current mechanism does not yet include SOA prediction capability.

Table A-7 in the Supplementary Materials gives the yields of aromatic oxidation products in the current mechanism that can be derived or estimated based on experimental yield measurements, and indicates how they were derived. The organic nitrate yields are assumed to increase with increasing carbon number, ranging from ∼8% for benzene up to a limit of ∼21%, and are estimated in a manner similar to that derived for the alkanes, corrected for aromatics based on the observed yield of benzyl nitrate from toluene (Calvert et al., 2002). However, the measured or estimated yields of the products on Table A-7 are not sufficient to account for all the processes involved in the OH reactions of the aromatics, so additional processes must also occur. We assume that this is formation of di-unsaturated 1,6-dicarbonyl products and OH radicals, in a process whose relative importance is independent of NO_x, shown as process "E" in Fig. 1a. This is probably an oversimplification, but it is necessary to assume that the relative importance of the additional process is independent of NO_x for the model to simulate chamber data and be consistent with available product yield data, which rules out competitions between reactions with NO and unimolecular reactions for the initially formed aromatic−OH−O_2 adducts. Assuming direct formation of OH radicals results in better model predictions of direct reactivity measurement data of Carter and Malkina (2002).
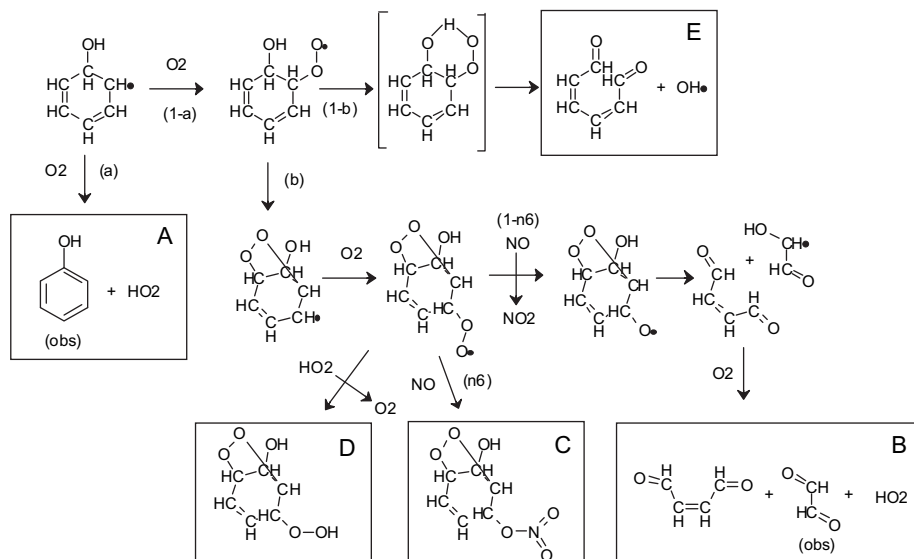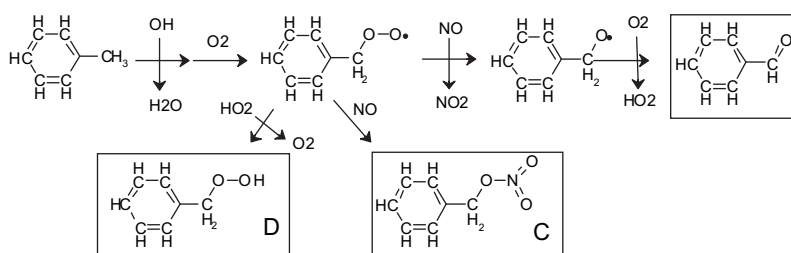
Fig. 1. General features of the aromatic reactions that are assumed in the current mechanism. The examples shown are for benzene and toluene, but analogous reactions are assumed for other alkylbenzenes.

The model species AFG1 and AFG2 are used to represent the monounsaturated 1,4-dicarbonyl ring-opening products formed as co-products from the α-dicarbonyls. These dicarbonyls with at least one aldehyde group are believed to be highly photoreactive (Calvert et al., 2002), and are assumed to account for the all the additional radical sources needed for models to simulate aromatic reactivity in environmental chamber experiments. The quantum yields for photolysis to form radical products are adjusted based on simulations of environmental chamber data with the individual aromatic compounds, using AFG1 to represent photolysis forming radicals and AFG2 for photodecomposition not forming radicals, with the relative yields adjusted to simulate the chamber data. The model species AFG3 is used to represent the di-unsaturated 1,6-dicarbonyls formed in the other assumed ring-opening route (process E in Fig. 1a), which are believed not to be as photoreactive, as well as the monounsaturated 1,4-diketones formed from para-substituted aromatics, which are also believed not to undergo rapid photodecomposition (Calvert et al., 2002). Table A-1 gives the reactions used for these model species and discusses how they were derived.

The mechanisms used for the other aromatic products are also given in Table A-1. In general, the mechanisms are similar as used for these products in SAPRC-99 (Carter, 2000a), though with some updates. Note that phenol and cresols are now represented by a single model species, whose mechanism has not been updated in this work because of problems simulating available chamber data (see footnote 51 to Table A-1). On the other hand, the formation of

HONO as a minor product in the nitrophenol photolysis has been included, based on the data of Bejan et al. (2006).

4.3. Mechanisms for other compounds

There are a number of other types of compounds besides alkylbenzenes for which estimated mechanisms could not be derived by the mechanism generation software, and whose mechanisms had to be derived or approximated based on compound-specific considerations. These include styrenes, naphthalenes, non-hydrocarbon aromatics such as chlorobenzenes, benzoates and pthallates, etc., furans, N-methyl-2-pyrrolidone and other nitrogen-containing organics, DMSO, bromides, siloxane compounds, and various pesticides. The derivations of the mechanisms for those compounds are summarized in Table A-5.

4.4. Lumped molecule representations

A number of compounds do not have separate mechanistic assignments in the mechanism, but instead are represented by assuming that they have the same per-molecule atmospheric impact as another compound. This is used for compounds whose reactivities or impacts are of interest but where the mechanistic difference with the representing compound is considered to be small compared to the uncertainty of the mechanism and for unspeciated mixtures of isomers where a compound or group of compounds are taken as representative. The lumped molecule

representations used in the current mechanism are given in Table A-8 in the Supplementary Materials.

4.5. Lumped VOC mechanisms for airshed models

Airshed model applications require simulations of highly complex mixtures of large numbers of VOCs, and in most cases it is not necessary or practical to represent each of them separately. For such applications, models with lumped model species that represent reactions of a large number of species with similar reaction rates and mechanisms are generally employed. These lumped model species are included with the species listing in Table 1. These include 9 lumped model species to represent VOCs in anthropogenic emissions (ALKn, OLEn, and AROn) and one to represent lumped biogenic terpenes (TERP).

The rate constants and product yield parameters in the lumped parameter species were derived from weighed averages of the corresponding parameters in the mechanisms of the individual compounds that each lumped species represented. The weighting factors were derived from the molar compositions of a mixture of VOCs taken as representative of those emitted in the model scenario (Carter, 2000b). In principle this mixture, and therefore the lumped species mechanisms, could be derived for each airshed model scenario, but the current practice is to use fixed parameter mechanisms derived as part of the mechanism development. For this mechanism, as with fixed parameter SAPRC-99 (Carter, 2000b), the parameters for the lumped species representing anthropogenic emissions were derived using the "Base ROG" mixture used to represent anthropogenic emissions from all sources in the reactivity scale calculations of Carter (1994a), while those for the lumped species representing terpenes were derived using the top 5 terpenes in the North American biogenic inventory from the NARSTO assessment of Guenther et al. (2000). The mixtures of compounds used to derive these lumped mechanisms are given in Table A-9, and the mechanisms are included in Table A-1 and Table A-2 in the Supplementary Materials.

5. Mechanism evaluation

The performance of the mechanism in simulating O_3 formation, rates of NO oxidation, and other measures of reactivity was evaluated by conducting model simulations of over 2400 environmental chamber experiments carried out in 11 different environmental chambers at 3 different institutions (Carter, 2010a). The chambers whose data were used for mechanism evaluation are summarized on Table A-10, the types of experiments are summarized on Table A-11, and the chamber effects parameters used when simulating these experiments are summarized in Table A-12 in the Supplementary Materials. Most of the experiments used for the evaluation were carried at the University of California at Riverside (UCR), but most experiments from the Tennessee Valley Authority (TVA) chamber and a few from the University of North Carolina (UNC) chamber were also included. Complete lists of the experiments, and input data for modeling are available on the SAPRC mechanism web site (Carter, 2010b).

The procedures used were the same as employed in previous evaluations of the RADM-2 (Carter and Lurmann, 1990), SAPRC-90 (Carter and Lurmann, 1991) and SAPRC-99 (Carter, 2000a, 2004) mechanisms. The most important and variable chamber effect is the "chamber radical source" first noted by Carter et al. (1982), which is attributed to offgassing of HONO (Brauers et al., 2003; Rohrer et al., 2004; Carter et al., 2005), and whose magnitudes must be determined by modeling appropriate characterization experiments (Carter et al., 1982, 2005; Carter and Lurmann, 1990, 1991; Carter, 2004). Note that the best fit HONO offgassing parameter values depend on the mechanism employed, with the rate constant for the $OH + NO_2$ reaction, the major termination process in the radical source characterization runs, being the most important.

The experiments used in this evaluation consist of characterization experiments used to derive or evaluate the chamber effects model, experiments used to evaluate mechanisms of individual VOCs, and mixture experiments. Experiments to evaluate individual VOC mechanisms consist of single VOC experiments where the VOC is irradiated by itself in the presence of NO_x, or in some cases with added CO or other reactant whose mechanism is known, and incremental reactivity experiments. Incremental reactivity experiments consist of two irradiations, usually carried out simultaneously in a dual reactor chamber: a "base case" experiment consisting of an irradiation of a reactive organic gas (ROG) surrogate − NO_x mixture approximating ambient chemical conditions, and irradiations of the same mixture with the test VOC added. (The ROG surrogates used are summarized in Table A-11, and generally consisted of mixtures of alkanes, alkenes, and aromatics with relative levels approximating ambient compositions.) The latter test the mechanisms' ability to predict the effects of the test compound on O_3 or other measures of air quality under somewhat more realistic chemical conditions, and are more useful than single VOC-NO_x experiments for compounds, such as alkanes, that do not have internal radical sources, because single VOC experiments with those compounds are highly sensitive to the chamber radical source (Carter et al., 1982). Mixture experiments are less useful for testing mechanisms of individual compounds, but are useful for testing mechanisms as a whole or in major portions.

In this work, the mechanism is evaluated primarily by determining its ability to simulate the amounts of O_3 formed and NO oxidized in the experiments. This is measured by $\Delta([O_3]-[NO])$, which is the change in $[O_3] − [NO]$ during the course of the experiment. As discussed previously (e.g., Carter and Atkinson, 1987; Carter and Lurmann, 1990, 1991), this gives a measure of the ability of the model to simulate the chemical processes that cause ozone formation even where ozone is suppressed by the presence of excess NO. The results of the incremental reactivity experiments were also used to evaluate the ability of the mechanism to simulate the effects of test compound on integrated OH radical levels, or IntOH. This is calculated from the rates of consumption of the most reactive VOC in the base case mixture that reacts only with OH radicals (usually m-xylene but sometimes n-octane, 1,3,5-trimethylbenzene or other compounds). This is useful because the effect of a VOC on overall radical levels affects the amounts of reaction and O_3 impacts of all the other VOCs that are present.

Representative results of the mechanism evaluation against chamber data are shown in Figs. 2 and 3. (See Table A-10 in the Supplementary Materials for descriptions of the chambers used and Table A-11 for a summary of the types of experiments.) Fig. 2a and b shows hourly average and standard deviations of the $\Delta([O_3]-[NO])$ model errors for all the single VOC experiments and all the mixture experiments, respectively. (Model errors in this case are defined as [calculated − experimental]/experimental values. Final model error is the model error at the end of the experiment.) Examples of plots of model errors against time for various types of experiments for two compounds with a large number of experiments are shown in Fig. 2c and Fig. 3 shows plots of experimental and calculated $\Delta([O_3]-[NO])$ and IntOH incremental reactivities for representative incremental reactivity experiments. (Incremental reactivities are changes in $\Delta([O_3]-[NO])$ and IntOH values caused by adding the VOC to the base case experiment, divided by the amount of test compound added.) Carter (2010a) gives similar model error vs. time and model error distribution plots for all the types of single VOC and mixture experiments, and gives plots of experimental and calculated $\Delta([O_3]-[NO])$ and IntOH reactivity data for all the incremental reactivity experiments that were modeled.
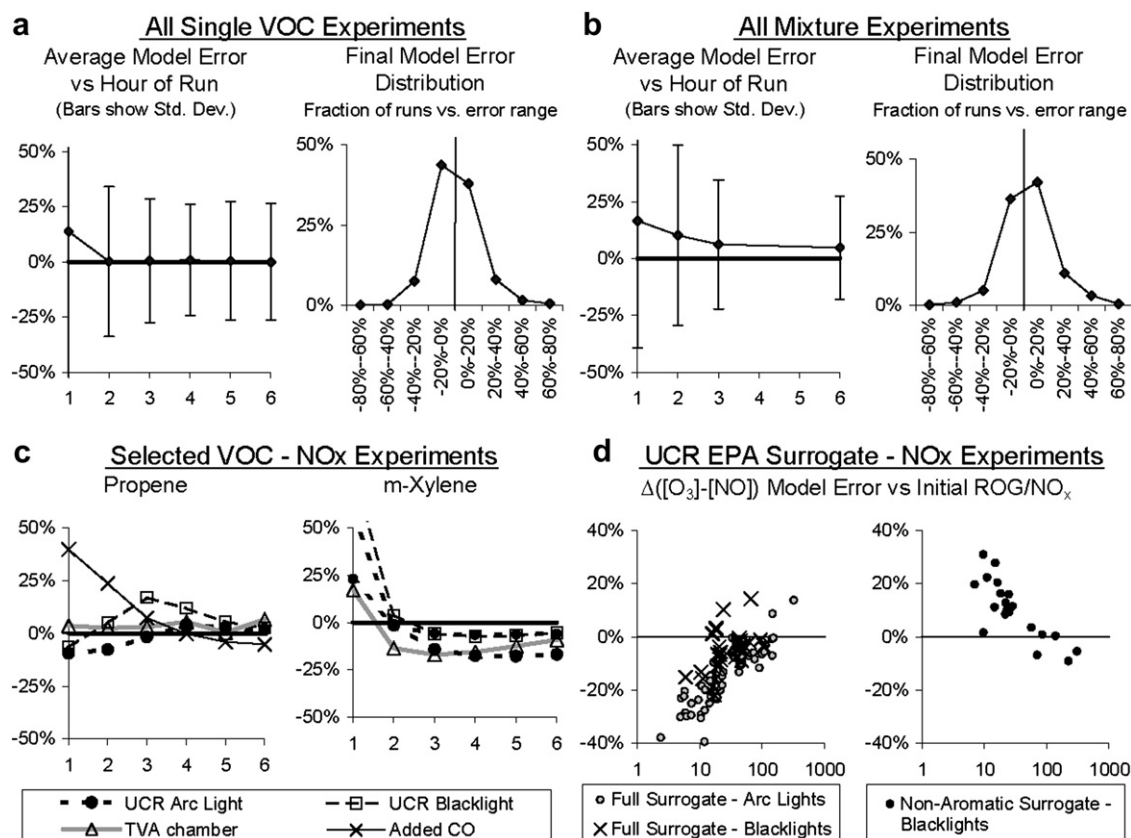
Fig. 2. Selected mechanism evaluation results for representative types of single VOC or mixture experiments (see Table A-10 for descriptions of the chambers used and Table A-11 for a summary of the types of experiments).

Table A-6 in the Supplementary Materials lists all the types of VOCs whose mechanisms were evaluated against chamber data, indicates the number of single VOC and incremental reactivity experiments, and gives the average $\Delta([O_3]-[NO])$ and $\Delta([O_3]-[NO])$ and IntOH reactivity model errors for each. The table also indicates those cases where the VOC mechanisms were adjusted to reduce biases in the simulations of these chamber data, and indicates the types of adjustments that were made. In most cases, the adjustments

were made based on subjective assessments of quality of model fits to $\Delta([O_3]-[NO])$ data. Most of the adjustments involved changing the overall nitrate yields in the peroxy + NO reactions to within their level of uncertainty, though in some cases other parameters were adjusted, and in a few cases fully parameterized mechanisms were derived and adjusted to fit these data. Examples of other adjusted parameters concerned quantum yields for photoreactive products from aromatics (discussed above), the total radical input in some O_3
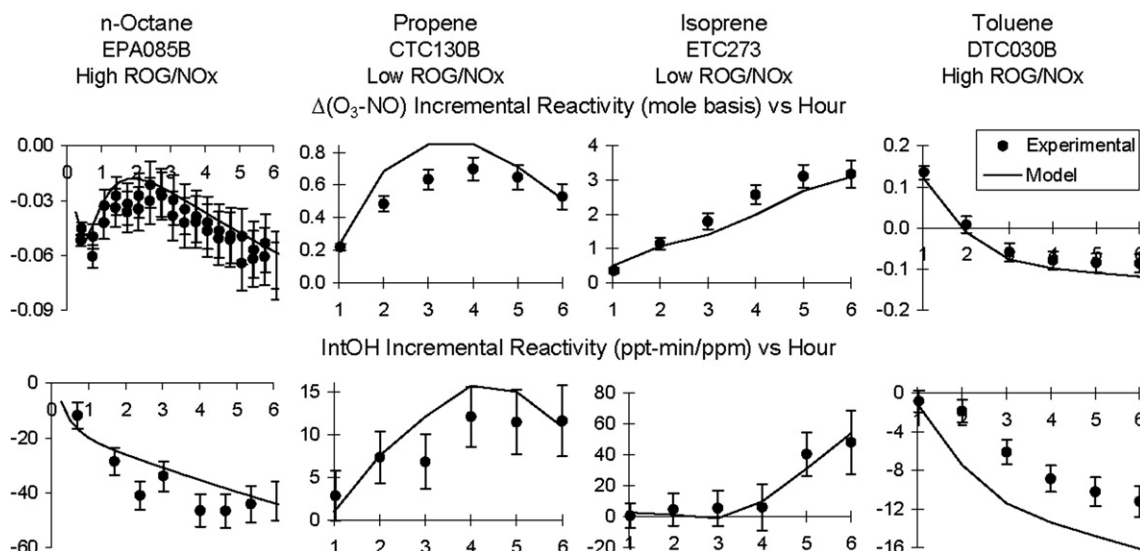

Fig. 3. Selected mechanism evaluation results for selected representative incremental reactivity experiments.

and $O^3P +$ alkene reactions, and overall quantum yields for some photoreactive compounds such as acrolein, methacrolein, and various ketones.

Fig. 2a and b show that there is very little overall bias in simulating the full sets of these experiments, but there is run-to-run scatter in the model errors, being on the order of ±25% by the end of the experiment. The low overall bias for the single compound experiments results at least in part from the fact that in many cases adjustments were made to mechanisms to remove biases in the simulations, as indicated in Table A-6. All but two VOCs (β-pinene and tetralin) had better than ±25% average Δ([O₃]-[NO]) model errors for the single compound runs; over 90% of the VOCs had average incremental reactivity model errors better than ±15% for Δ([O₃]-[NO]) and better than ±20% for IntOH. This is similar to the results of the evaluation of the SAPRC-99 mechanism (Carter, 2000a), except that a much larger number of runs and types of VOCs are modeled with this updated mechanism. The compounds with worse average biases either had only a limited number of experiments or experiments considered likely to have problems, or problems with the mechanisms as indicated in the footnotes to Table A-6 and by Carter (2010a, and references therein).

The mixture experiments in the evaluation dataset include a large number of ambient ROG surrogate − NOₓ experiments carried out at a variety of initial ROG and NOₓ levels approaching ambient concentration ranges in the new UCR EPA chamber with the arc light source (Carter et al., 2005). The SAPRC-99 mechanism was found to have a consistent bias in underpredicting Δ([O₃]-[NO]) at low ROG/NOₓ levels in those experiments, with the model error being correlated with the ROG/NOₓ ratio (Carter, 2000a; Carter et al., 2005). Fig. 2d shows that this is still the case with the SAPRC-07 mechanism. Additional surrogate − NOₓ experiments have been conducted more recently, including experiments using blacklights and experiments using the ROG surrogate with the aromatics removed. Fig. 2d shows that changing the light source does not change the nature of the bias, but that removing the aromatics from the ROG surrogate causes the bias to have the opposite dependence on ROG/NOₓ. Therefore, the underprediction bias at low ROG/NOₓ ratios is likely related to problems with the aromatics mechanisms. This problem has not been resolved when updating the mechanism from SAPRC-99 to SAPRC-07, despite the improvements in the aromatics mechanisms in other respects. The cause of this problem is unknown at the present time, but it may be related to a tendency of the current aromatics mechanisms to underpredict radical levels, even after adjustments to fit ozone.

6. Updated ozone reactivity scales

One of the major applications of the SAPRC mechanisms is calculation of ozone reactivity scales for VOCs, including the Maximum Incremental Reactivity (MIR) scale that is used or being considered for use in regulatory applications in California (CARB, 1993, 2000, 2009). This and other reactivity scales have been updated to SAPRC-07 as part of this work, with a large number of VOCs not in the SAPRC-99 scales being added.

The methods, scenarios, and reactivity scales that were used in this reactivity scale update are the same as employed previously for the previous SAPRC-90 (Carter, 1994a) and SAPRC-99 scales (Carter, 2000a, 2003). These are based on 39 single-day "base case" box model scenarios (EPA, 1984; Carter, 1994b) derived by the EPA for assessing how various ROG and NOₓ control strategies would affect ozone nonattainment in various areas of the country (Baugues, 1990). For the purpose of deriving reactivity scales for specified chemical conditions, the NOₓ inputs in these scenarios are adjusted to yield maximum incremental reactivities of the base ROG mixture for calculation of the MIR scale, or to yield maximum ozone concentration for calculation of the Maximum Ozone Incremental Reactivity (MOIR) scale, or to yield equal relative sensitivity of O₃ to changes in total VOC or total NOₓ emissions for calculation of the Equal Benefit Incremental Reactivity (EBIR) scales (Carter, 1994a, 2000a, 2010a). The MIR scale represents relatively high NOₓ conditions that are most sensitive to VOC emissions; the MOIR scale represents lower NOₓ conditions that are most favorable for ozone formation; and the EBIR scale represents the lowest NOₓ conditions where VOC control is at least as effective in reducing ozone as NOₓ control.

Table A-5 in the Supplementary Materials lists the ozone reactivities of all the types of VOCs represented in the SAPRC-07 mechanism in the MIR, MOIR, and EBIR scales. It also gives subjective uncertainty codes and estimates of possible biases, if any, in the calculated ozone reactivity values. The changes in the MIR values caused by this update of the SAPRC mechanism are shown in Fig. 4, which shows a plot of the incremental reactivities in the updated scale against those in the latest SAPRC-99 scale provided by Carter (2003). The 1:1 and ±30% lines are also shown. The average change in the MIRs (excluding the outliers where the change was greater than 50%) was −12%, and the average absolute magnitude of the change (again excluding the outliers) was 14%. The change was less than 30% for approximately 93% of these VOCs. The MIR for the base ROG mixture, which can be used as the standard for relative
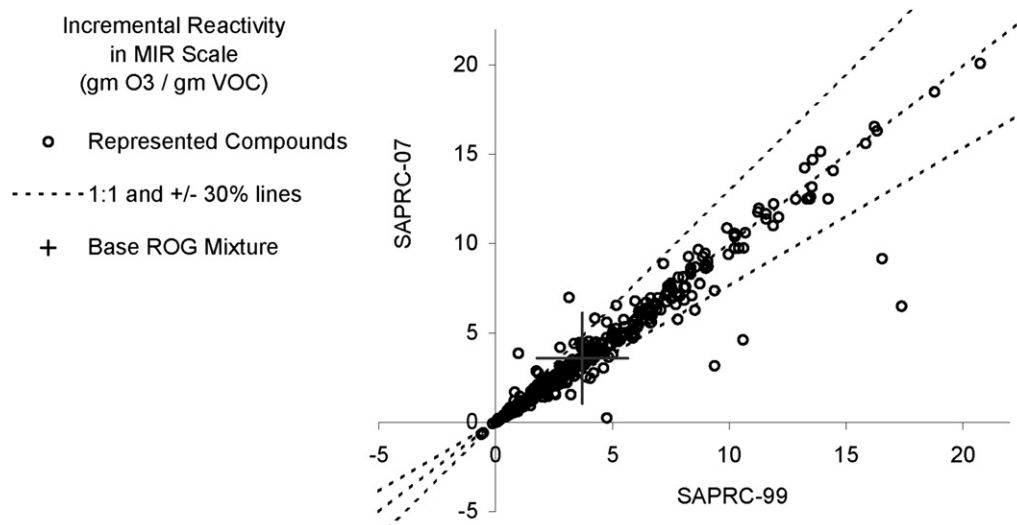

Fig. 4. Plots of incremental reactivities in the MIR scale computed using the updated mechanism against those reported previously by Carter (2003).
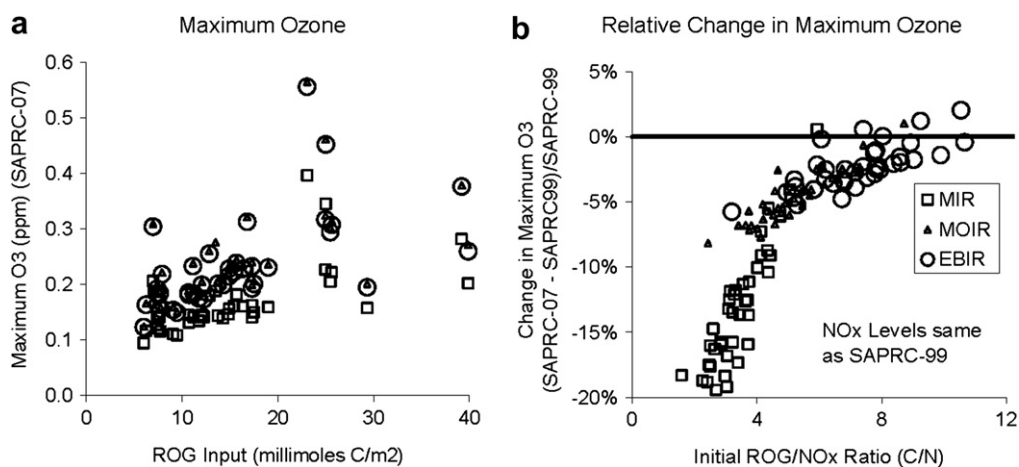
Fig. 5. Plots of (a) maximum ozone concentrations calculated by SAPRC-07 and (b) changes in maximum ozone concentrations caused by the mechanism update from SAPRC-99 to SAPRC-07 for the 1-day scenarios used for reactivity scale calculations.

reactivity scales, decreased by about 2%. If this is taken into account, the average change in relative MIR values would be approximately 10%, excluding the outliers.

The compounds whose MIR values changed by more than 30%, and the probable reasons for the changes, are listed in Table A-13 in the Supplementary Materials. Excluding 3-methoxy-1-butanol, which had a factor of ~3 MIR increase because the SAPRC-99 mechanism had a factor of 10 error in the OH rate constant, the greatest changes were for amines, for which new mechanisms were derived based on new chamber data by Carter (2008), and for halogenated compounds, because of the higher estimated photolysis rates for the chloroaldehyde and chloroketone products predicted to be formed and the improved representation of chlorine chemistry. For all other compounds the change in MIR values was no greater than ~65%. This suggests a probable maximum likely MIR change that may occur for compounds for which no mechanism evaluation data are available.

7. Ambient ozone predictions

The other major application of the updated mechanism will be use in airshed models to predict effects of emissions on formation of ozone and other secondary pollutants. An indication of the effect of the mechanism update can be made by comparing ozone predictions in the 1-day scenarios used to calculate the reactivity scales discussed above. Fig. 5a shows plots of maximum O_3 concentrations for the reactivity scenarios using the current mechanism against total ROG input. Note that some scenarios have O_3 levels as high as 500 ppb or more, suggesting that the scenarios should be updated to reflect present conditions, which is beyond the scope of this project. However, at least they represent a range of chemical conditions that can give an initial indication of the effects of mechanism updates on one-day O_3 predictions.

Fig. 5b shows plots of relative changes maximum ozone concentrations resulting from the mechanism update against the ROG/NO_x ratio for the scenarios used for reactivity assessment. Note that the NO_x levels in the MIR, MOIR, and EBIR are derived by adjustments to achieve desired reactivity conditions, so in general they depend on the mechanism employed. To place the comparisons on an equal NO_x basis, the SAPRC-07 calculations on Fig. 5b were made using the NO_x levels of the SAPRC-99 scenarios. The mechanism update generally causes reductions in the predicted maximum ozone levels, with the changes being small at high ROG/NO_x ratios, and increasing as the ROG/NO_x ratio is reduced, with the reduction being as much as ~20% in some of the MIR scenarios. If the NO_x

levels in the SAPRC-07 calculations are adjusted to yield MIR, MOIR, or EBIR conditions for this mechanism (as was done when deriving the reactivity scales), the distribution of relative O_3 changes become about the same for each of the three types of scenarios, ranging from ~0% to ~−7%, depending on the ROG/NO_x ratio.

The increase in the rate constant for the OH + NO_2 reaction may be a factor in causing the generally lower O_3 predictions resulting from the mechanism update at low ROG/NO_x ratios, though this needs to be assessed. The effect of the update may be different in the more realistic 3-D model scenarios that are generally used in air quality planning and research studies.

8. Peer review of mechanism

Because of its proposed use for regulatory applications, the California Air Resources Board contracted four research groups to carry out a peer review of various aspects of the mechanism. These reviews, and the responses to them, are summarized briefly below.

Derwent et al. (2008) focused on comparing incremental ozone impacts of 121 selected compounds calculated using SAPRC-07 and the Master Chemical Mechanism (v. 3.1). Their general conclusion was that for most compounds the ozone impacts calculated using the two mechanisms were consistent with each other, though there were significant differences for certain compounds. These are attributed to different assumptions and approximations being made for certain compounds (Carter, 2009a).

Azzi et al. (2008) focused on comparing the ability of the SAPRC-07 mechanism, and also SAPRC-99 and MCM 3.1, to simulate the results of isoprene, toluene, m-xylene, and evaporated fuel environmental chamber experiments carried out in the CSIRO chamber. In general, SAPRC-07 performed reasonably well in simulating these data given the uncertainties in evaluating mechanisms against chamber data, particularly with complex mixtures. There is some indication of problems with the toluene mechanism that merits further investigation, and some complex mixture experiments were simulated better using SAPRC-99 than SAPRC-07.

Harley (2009) discussed implementing the mechanism in 3-D modeling, and brings up several issues that need to be addressed. These include the need to develop a version of the mechanism for sensitivity studies on the uncertain and important OH + NO_2 rate constant, and the need to update the base ROG mixture used to derive the fixed parameter version of the mechanism.

Stockwell (2009) gave a detailed comparison of the individual chemical reactions and rate constants in various current mechanisms

and commented on differences and his assessment of their chemical reasonableness and the extent to which they represent the state of the science. Overall, he concludes that SAPRC-07 represents the current state of the science and he comments favorably about certain aspects of the mechanism, but he had several criticisms and recommendation. Some of his comments resulted in revealing several errors that had to be corrected.

The responses to these reviews are given by Carter (2009a). The reviews of Derwent et al. (2008), Azzi et al. (2008) and Stockwell (2009) indicated areas where future work and intercomparisons with other mechanisms are needed, but in most cases did not indicate a clear need to change SAPRC-07 at the present time. The review by Stockwell resulted in several changes to the base mechanism being made to correct errors and to remove the unnecessary HO_2 + formaldehyde reaction. Most differences between SAPRC-07 and the mechanisms of Derwent et al. (2008) and Stockwell (2009) reflect differences in chemical judgment and areas where future mechanism development work is needed. Model implementation and sensitivity work recommended by Harley (2009) is beyond the scope of this paper but is planned or underway.

9. Discussion

This project succeeded in providing a complete update to the SAPRC-99 mechanism that represents the current state of the science. Although adapting this mechanism for use in SOA predictions is beyond the scope of this project, the capability for adaptation to SOA predictions was improved by incorporating a more explicit representation of peroxy + peroxy and hydroperoxide formation. This mechanism was comprehensively evaluated against the available environmental chamber database from the UCR and TVA chambers, and in most cases was found to perform as well as can reasonably be expected given the current state of the science. Evaluations against the full UNC chamber database still needs to be done, but based on results of evaluations of other mechanisms using this database (Carter and Lurmann, 1990, 1991; Whitten et al., 2010) the mechanism performance is expected to be similar. This mechanism was used to completely update the MIR and other ozone reactivity scales, so these scales now represent the current state of the science, at least in their chemical basis.

Work is beginning on implementing and using this mechanism in urban and regional airshed models for research and regulatory applications. Implication in current models is complicated by the fact that the revised peroxy radical treatment requires some changes to airshed model software. A condensed version of this mechanism has been developed that is simpler to implement (Carter, 2010c,d), and emissions and speciation assignments have been made for this and the condensed versions (Carter, 2009b).

Although progress has been significant, additional work remains. The impacts of the increase in the important $OH + NO_2$ rate constant and other uncertainties in the base mechanism need to be investigated. The base ROG mixture used to derive the parameters in the condensed mechanism for airshed models needs to be updated, as do the scenarios and methodology used for deriving the ozone reactivity scales. While the aromatics mechanisms have been improved, they are not satisfactory in all respects in terms of consistency with available laboratory and chamber data and significant uncertainties remain. Uncertainties also remain in the mechanisms for a number of other types of VOCs, and for some applications additional halogens beside chlorine may need to be represented. Finally, the mechanism needs to be adapted, expanded and evaluated for predicting secondary organic aerosol formation.

The files needed to implement the mechanism and additional documentation is available at the SAPRC mechanism web site at http://www.cert.ucr.edu/~carter/SAPRC.

Appendix. Supplementary information

Supplementary data associated with this article can be found in the online version at doi:10.1016/j.atmosenv.2010.01.026.

References

Arey, J., Obermeyer, G., Aschmann, S.M., Chattopadhyay, S., Cusick, R.D., Atkinson, R., 2009. Dicarbonyl products of the OH radical-initiated reaction of a series of aromatic hydrocarbons. Environ. Sci. Technol. 43, 683–689.

Azzi, M., White, S., Angove, D., November 2008. Review of the SAPRC-07 Chemical Mechanism. Report to the California Air Resources Board. Available at: http://www.arb.ca.gov/research/reactivity/rsac.htm.

Bergin, M., Noblet, G.S., Petrini, K., Dhieux, J.R., Milford, J.B., Harley, R.A., 1999. Formal uncertainty analysis of a Lagrangian photochemical air pollution model. Environ. Sci. Technol. 33, 1116–1126.

Barnes, I., 2006. Mechanisms of the photoxidation of aromatic hydrocarbons: chemistry of ring-retaining products. In: Presented at the International Conference on Atmospheric Chemical Mechanisms, Davis CA, December 6–8. See http://www.cert.ucr.edu/~carter/Mechanism_Conference.

Baugues, K., January 1990. Preliminary Planning Information for Updating the Ozone Regulatory Impact Analysis Version of EKMA. Draft Document. Source Receptor Analysis Branch, Technical Support Division, U.S. Environmental Protection Agency, Research Triangle Park, NC.

Bejan, Y., Abd el Aal, I., Barnes, T., Benter, B., Bohn, P., WiesenKleffmann, J., 2006. The photolysis of ortho-nitrophenols: a new gas-phase source of HONO. Phys. Chemis. Chem. Phys. 8, 2028–2035.

Brauers, T., Bohn, B., Johnen, F.-J., Rohrer, F., Rodriguez Bares, S., Tillmann, R., Wahner, A., 2003. The atmosphere simulation chamber SAPHIR: a tool for the investigation of photochemistry. In: Presented at the EGS–AGU–EUG Joint Assembly, Nice, France, April 11, 2003. See also http://www.fz-juelich.de/icg/icg-ii/saphir/home.

Calvert, J.G., Atkinson, R., Becker, K.H., Kamens, R.M., Seinfeld, J.H., Wallington, T.J., Yarwood, G., 2002. The Mechanisms of Atmospheric Oxidation of Aromatic Hydrocarbons. Oxford University Press, New York.

CARB, 1993. Proposed Regulations for Low-emission Vehicles and Clean Fuels – Staff Report and Technical Support Document. California Air Resources Board, Sacramento, CA. August 13, 1990. See also Appendix VIII of "California Exhaust Emission Standards and Test Procedures for 1988 and Subsequent Model Passenger Cars, Light Duty Trucks and Medium Duty Vehicles," as last amended September 22, 1993. Incorporated by reference in Section 1960.

CARB, May 5, 2000. Initial Statement of Reasons for the Proposed Amendments to the Regulation for Reducing Volatile Organic Compound Emissions from Aerosol Coating Products and Proposed Tables of Maximum Incremental Reactivity (MIR) Values, and Proposed Amendments to Method 310, 'Determination of Volatile Organic Compounds in Consumer Products'. California Air Resources Board, Sacramento, CA.

CARB, 2009. Air resources board reactivity programs. http://www.arb.ca.gov/research/reactivity/reactivity.htm Web page at;Last updated May 21.

Carter, W.P.L., 1994a. Development of ozone reactivity scales for volatile organic compounds. J. Air & Waste Manage. Assoc. 44, 881–899.

Carter, W.P.L., April 12, 1994b. Calculation of reactivity scales using an updated carbon bond IV mechanism. Report Prepared for Systems Applications International Under Funding from the Auto/Oil Air Quality Improvement Research Program, Available at: http://www.cert.ucr.edu/~carter/absts.htm#cb4rct.

Carter, W.P.L., May 8, 2000a. Documentation of the SAPRC-99 chemical mechanism for VOC reactivity assessment. Report to the California Air Resources Board, Contracts 92-329 and 95-308. Available at: http://cert.ucr.edu/~carter/absts.htm#saprc99 and http://www.cert.ucr.edu/~carter/reactdat.htm.

Carter, W.P.L., January 29, 2000b. Implementation of the SAPRC-99 chemical mechanism into the models-3 framework. Report to the United States Environmental Protection Agency. Available at: http://www.cert.ucr.edu/~carter/absts.htm#s99mod3.

Carter, W.P.L., 2003. The SAPRC-99 chemical mechanism and updated VOC reactivity scales, updated and corrected data as of February 5, 2003. Available at: http://www.cert.ucr.edu/~carter/reactdat.htm.

Carter, W.P.L., May 5, 2004. Evaluation of a gas-phase atmospheric reaction mechanism for low NO_x conditions. Final Report to California Air Resources Board Contract No. 01-305. Available at: http://www.cert.ucr.edu/~carter/absts.htm#lnoxrpt.

Carter, W.P.L., February 19, 2008. Reactivity estimates for selected consumer product compounds. Final Report to the California Air Resources Board Contract 06-408. Available at: http://www.cert.ucr.edu/~carter/absts.htm#aminrep.

Carter, W.P.L., March 20, 2009a. Peer review of the SAPRC-07 chemical mechanism: response to reviewers' comments. Prepared for California Air Resources Board Contract 07-730. Available at: http://www.cert.ucr.edu/~carter/SAPRC.

Carter, W.P.L., 2009b. Current project information page: development of an improved chemical speciation database for processing emissions of volatile organic compounds for air quality models. Web page available at: http://www.cert.ucr.edu/~carter/emitdb/ Last updated April 30.

Carter, W.P.L., January 27, 2010a. Development of the SAPRC-07 chemical mechanism and updated ozone reactivity scale. Revised final report to the California Air Resources Board Contract No. 03-318. Available at: http://www.cert.ucr.edu/~carter/SAPRC.

Carter, W.P.L., 2010b. SAPRC atmospheric chemical mechanisms and voc reactivity scales. Web page at: http://www.cert.ucr.edu/~carter/SAPRC Last updated February 2.

Carter, W.P.L., January 28, 2010c. Development of a condensed SAPRC-07 chemical mechanism. Final Report to the California Air Resources Board. Available at: http://www.cert.ucr.edu/~carter/absts.htm#csaprc07.

Carter, W.P.L., 2010d. Development of a condensed SAPRC-07 chemical mechanism. Atmos. Environ. 44, 5336–5345.

Carter, W.P.L., Atkinson, R., Winer, A.M., Pitts Jr., J.N., 1982. Experimental investigation of chamber-dependent radical sources. Int. J. Chem. Kinet. 14, 1071.

Carter, W.P.L., Atkinson, R., 1987. An experimental study of incremental hydrocarbon reactivity. Environ. Sci. Technol. 21, 670–679.

Carter, W.P.L., Lurmann, F.W., 1990. Final Report, EPA-600/3-90-001. Evaluation of the RADM gas-phase chemical mechanism.

Carter, W.P.L., Lurmann, F.W., 1991. Evaluation of a detailed gas-phase atmospheric reaction mechanism using environmental chamber data. Atmos. Environ. 25A, 2771–2806.

Carter, R., Atkinson, W.P.L., 1996. Development and evaluation of a detailed mechanism for the atmospheric reactions of isoprene and NO_x. Int. J. Chem. Kinet. 28, 497–530.

Carter, W.P.L., Luo, D., Malkina, I.L., May 19, 1997. Investigation of that atmospheric reactions of chloropicrin. Atmos. Environ. 31, 1425–1439. See also Report to the Chloropicrin Manufacturers Task Group. Report available at: http://www.cert.ucr.edu/~carter/absts.htm#clpicrin.

Carter, W.P.L., Malkina, I.L., May 22, 2002. Development and application of improved methods for measurement of ozone formation potentials of volatile organic compounds. Final report to California Air Resources Board Contract 97-314. Available at: http://www.cert.ucr.edu/~carter/absts.htm#rmethrpt.

Carter, W.P.L., Cocker III, D.R., Fitz, D.R., Malkina, I.L., Bumiller, K., Sauer, C.G., Pisano, J.T., Bufalino, C., Song, C., 2005. A new environmental chamber for evaluation of gas-phase chemical mechanisms and secondary aerosol formation. Atmos. Environ. 39, 7768–7788.

Carter, W.P.L., Malkina, I.L., January 10, 2007. Investigation of the atmospheric impacts of selected pesticides. Final Report to the California Air Resources Board Contract 04-334. Available at: http://www.cert.ucr.edu/~carter/absts.htm#pestrep.

Derwent, R.G., Jenkin, M.E., Saunders, S.M., Pilling, M.J., 1998. Photochemical ozone creation potentials for organic compounds in northwest Europe calculated with a master chemical mechanism. Atmos. Environ. 32, 2429–2441.

Derwent, R.G., Jenkin, M.E., Pilling, M.J., 2008. Reactivity scales ad comparative tools for chemical mechanisms: SAPRC vs. MCM. Final Report to the California Air Resources Board. Available at: http://www.arb.ca.gov/research/reactivity/rsac.htm.

Dodge, M.C., 2000. Chemical oxidant mechanisms for air quality modeling, critical review paper for 1998 ozone assessment. Atmos. Environ. 34, 2103–2130.

EPA, February 1984. Guideline for using the carbon bond mechanism in city-specific EKMA. EPA-450/4-84-005.

Gery, M.W., Whitten, G.Z., Killus, J.P., January 1988. Development and testing of the CBM-IV for urban and regional modeling. EPA-600/3-88-012.

Guenther, A., Geron, C., Pierce, T., Lamb, B., Harley, P., Fall, R., 2000. Natural emissions of non-methane volatile organic compounds, carbon monoxide, and oxides of nitrogen from North America. Atmos. Environ. 34, 2205–2230.

Harley, R., 2009. SAPRC-07 chemical mechanism peer review comments. Report to the California Air Resources Board. Available at: http://www.arb.ca.gov/research/reactivity/rsac.htm.

Hurley, M.D., Sokolov, O., Wallington, T.J., Takekawa, H., Karasawa, M., Klotz, B., Barnes, I., Becker, K.H., 2001. Organic aerosol formation during the atmospheric degradation of toluene. Environ. Sci. Technol. 35 (7), 1358–1366.

Jenkin, M.E., Saunders, S.M., Pilling, M.J., 1997. The tropospheric degradation of volatile organic compounds: a protocol for mechanism development. Atmos. Environ. 31 (1), 81–104.

Jenkin, M.E., Saunders, S.M., Wagner, V., Pilling, M.J., 2003. Protocol for the development of the Master Chemical Mechanism, MCM v3 (part B): tropospheric degradation of aromatic volatile organic compounds. Atmos. Chem. Phys. 3, 181–193.

NASA, July 2006. Chemical Kinetics and Photochemical Data for Use in Stratospheric Modeling, Evaluation Number 15. JPL Publication 06-2. Jet Propulsion Laboratory, Pasadena, California.

Odum, J.R., Hoffmann, T., Bowman, F., Collins, D., Flagan, R.C., Seinfeld, J.H., 1996. Gas/particle partitioning and secondary organic aerosol yields. Environ. Sci. Technol. 30 (8), 2580–2585.

Rohrer, F., Bohn, B., Brauers, T., Brüning, D., Johnen, F.-J., Wahner, A., Kleffmann, J., 2004. Characterisation of the photolytic HONO-source in the atmosphere simulation chamber SAPHIR. Atmos. Chem. Phys. Disc. 4, 7881–7915.

Saunders, S.M., Jenkin, M.E., Derwent, R.G., Pilling, M.J., 2003. Protocol for the development of the Master Chemical Mechanism, MCM v3 (part A): tropospheric degradation of non-aromatic volatile organic compounds. Atmos. Chem. Phys. 3, 161–180.

Sarwar, G., Luecken, D., Yarwood, G., Whitten, G.Z., Carter, W.P.L., 2008. Impact of an updated carbon bond mechanism on predictions from the Community Multiscale Air Quality (CMAQ) modeling system: preliminary assessment. J. Appl. Met. Climat. 47, 3–14.

Sato, K., Klotz, B., Hatakeyama, S., Imamura, T., Washizu, Y., Matsumi, Y., Washida, N., 2004. Secondary organic aerosol formation during the photooxidation of toluene: dependence on initial hydrocarbon concentration. B Chem Soc Jpn 77 (4), 667–671.

Song, C., Na, K.S., Cocker, D.R., 2005. Impact of the hydrocarbon to NO_x ratio on secondary organic aerosol formation. Environ. Sci. Technol. 39 (9), 3143–3149.

Stockwell, W.R., Middleton, P., Chang, J.S., Tang, X., 1990. The second generation regional acid deposition model chemical mechanism for regional air quality modeling. J. Geophys. Res. 95, 16343–16376.

Stockwell, W.R., Kirchner, F., Kuhn, M., Seefeld, S., 1997. A new mechanism for regional atmospheric chemistry modeling. J. Geophys. Res. 102, 25847–25880.

Stockwell, W.R., November 29, 1999. Review of the updated maximum incremental reactivity scale of Dr. William Carter. Report to the California Air Resources Board Contract No. 98-401, Sacramento, California. Available at: http://www.cert.ucr.edu/~carter/reactdat.htm.

Stockwell, W.R., March 9, 2009. Peer review of the SAPRC-07 chemical mechanism of Dr. William Carter. Draft report to the California Air Resources Board. Available at: http://www.arb.ca.gov/research/reactivity/rsac.htm.

Tanaka, P.L., Riemer, D.D., Chang, S., Yarwood, G., McDonald-Buller, E.C., Apel, E.C., Orlando, J.J., Silva, P.J., Jimenez, J.L., Canagaratna, M.R., Neece, J.D., Mullins, C.B., Allen, D.T., 2003. Direct evidence for chlorine-enhanced urban ozone formation in Houston, Texas. Atmos. Environ. 37, 1393–1400.

Whitten, G.Z., Heo, G., Kimura, Y., McDonald-Buller, E., Allen, D.T., Carter, W.P.L., Yarwood, G., 2010. A new condensed toluene mechanism for carbon bond: CB05-TU. Atmos. Environ. 44, 5346–5355.

Yarwood, G., Rao, S., Yocke, M., Whitten, G., 2005. Updates to the carbon bond chemical mechanism: CB05. Final report to the U.S. EPA, RT-0400675. Available at: www.camx.com.